

Equilibrium ranges in surf zone wave spectra

Jane McKee Smith

U.S. Army Engineer Research and Development Center, Vicksburg, Mississippi, USA

Charles L. Vincent

Office of Naval Research, Arlington, Virginia, USA

Received 25 April 2003; revised 4 August 2003; accepted 2 October 2003; published 26 November 2003.

[1] Laboratory measurements of two wave trains breaking on a plane slope demonstrate dramatic changes in spectral shape in the surf zone. The higher-frequency spectral peak is completely eliminated in the surf zone, and the resulting spectral shape is similar regardless of the peak frequency and relative energy content of the higher-frequency peak. Examination of both laboratory and field data show that surf zone wave number (k) spectra evolve to contain two equilibrium ranges. The higher-frequency range is similar to that proposed by Toba in deeper water with the form $k^{-5/2}$ and is valid for approximately $k > 1/\text{depth}$. The second range falls between the peak wave number and $k = 1/\text{depth}$ and has a wave number dependence of $k^{-4/3}$, similar to that proposed by Zakharov on theoretical grounds. The equilibrium range coefficients, which are a function of wind speed in deep and finite water depths, are a function of the water depth in the surf zone. The laboratory and field data sets used in these analyses covered a broad range of conditions (unidirectional and multidirectional waves, plane and barred beaches, two orders of magnitude variation in wave height, and one order of magnitude variation in wave period), yet the equilibrium ranges identified were consistent and provide a robust parameterization of surf zone wave spectra. *INDEX TERMS*: 4546 Oceanography: Physical: Nearshore processes; 4560 Oceanography: Physical: Surface waves and tides (1255); 4203 Oceanography: General: Analytical modeling; *KEYWORDS*: surf zone, wave spectra, equilibrium range, wave breaking, Field Research Facility, two-peaked spectra

Citation: Smith, J. M., and C. L. Vincent, Equilibrium ranges in surf zone wave spectra, *J. Geophys. Res.*, 108(C11), 3366, doi:10.1029/2003JC001930, 2003.

1. Introduction

[2] The concept of an equilibrium range in deepwater and finite depth wave spectra has evolved through dimensional analysis [Phillips, 1958], empirical observations [Toba, 1973; Donelan *et al.*, 1985], numerical simulations [Hasselmann, 1962; Resio, 1987], and theory [Zakharov and Filonenko, 1966; Kitaigorodskii, 1983]. Resio *et al.* [2001] show through direct numerical simulation that in deep and finite water depth, the equilibrium range of wave spectra relax to the form:

$$F(k) = \beta k^n \quad (1)$$

where F is energy density, k is wave number, and $n = -5/2$. Observations suggest equation (1) is valid for the region from 1.5 to $3 f_p$, where f_p is the peak frequency. At much higher frequencies there is some question as to whether it shifts to the k^{-3} (ω^{-5} , where ω is the radial frequency) form of Phillips [1958]. The equilibrium range was originally hypothesized to result from dissipation due to wave breaking [Phillips, 1958], but more recent publications attribute the

development of the equilibrium range to four-wave interactions [Kitaigorodskii, 1983; Resio *et al.*, 2001]. The nonlinear interactions transfer energy to high frequencies analogous to the Komolgorov cascade in turbulence spectra, and the equilibrium range develops because of a constant flux of energy. Numerical experiments have shown that perturbations artificially imposed in the equilibrium range are quickly smoothed through the four-wave interactions [Resio *et al.*, 2001]. Also, the four-wave interactions become substantially stronger as water depth decreases [Herterich and Hasselmann, 1980]. Although the mechanism that generates and maintains the equilibrium range has been documented only recently, the concept of the equilibrium range has been used for over 40 years in parametric descriptions of spectra. These parametric shapes have been used to interpret measurements, generate synthetic wave spectra, and reduce computations in numerical models. This research has focused on waves outside the surf zone.

[3] Thornton [1977] derived an equilibrium range for shallow water waves (assuming $c^2 = gd$, where c is wave celerity, g is gravitational acceleration, and d is water depth) using dimensional analysis and assuming wave celerity is the relevant parameter at wave breaking:

$$S(\omega) = \beta g d \omega^{-3} \quad (2)$$

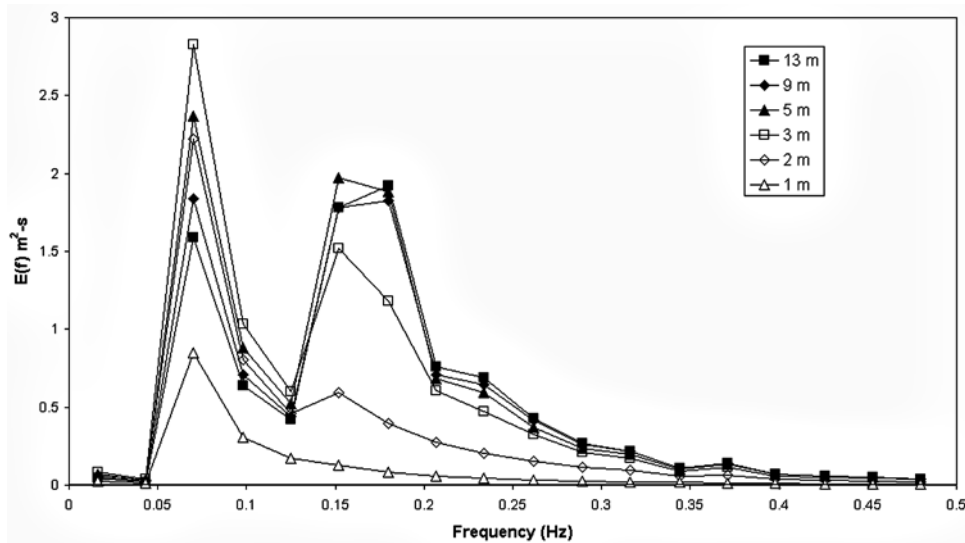


Figure 1. Two-peaked wave spectra measured at depths of 1, 2, 3, 5, 9, and 13 m from the FRF, Duck, North Carolina.

where S is the frequency spectrum and β is a constant. Thornton found that the equilibrium range always existed, even when the waves were not saturated (e.g., light winds and swell). Also, he states that it is not understood if the equilibrium range is a residual of a deeper water equilibrium range or caused by energy transfers due to nonlinear interactions. Thornton's experimental data, much of which was taken inside the surf zone, has a slope less steep than ω^{-3} . Thornton suggests the slope in the surf zone is approximately $\omega^{-7/3}$ because of surface tension effects as postulated by Phillips [1966]. Zakharov [1999] theoretically derived the equilibrium range for very shallow water waves from the wave kinetic equation and a Kolmogorov range hypothesis. His resulting equilibrium range shape is $\omega^{-4/3}$, which will occur around $kd < 0.3$. Zakharov does not provide field or laboratory measurements to confirm these results. In the region near $kd < 0.3$ for waves of small amplitude (typical of an equilibrium range component), ω is approximately gk ; thus $\omega^{-4/3}$ corresponds to $k^{-4/3}$.

[4] Smith and Vincent [1992] performed laboratory experiments of wave breaking for two superimposed wave trains in a laboratory flume. Their results showed that spectral shape changes dramatically in the surf zone for two-peaked spectra. The higher-frequency spectral peak was dissipated much faster than the lower-frequency peak in the surf zone. At the shallowest gauges, the high-frequency peak was completely eliminated. The preferential decay of the high-frequency peak occurred for cases with greater initial energy in the high-frequency peak, equal energy in the peaks, and greater energy in the low-frequency peak. Figure 1 shows field measurements from the U.S. Army Engineer Research and Development Center (ERDC) Field Research Facility (FRF) in Duck, NC that illustrates the same energy dissipation pattern in the ocean. Breaking algorithms implemented in phase-averaged spectra wave models [e.g., Booij *et al.*, 1999; Smith *et al.*, 2001] dissipate energy as a function of frequency in proportion to the relative energy density at each frequency. This method does not represent the

observed dissipation pattern or the resulting spectral shape for multiple peaked spectra.

[5] Boussinesq models have been extended to the surf zone using empirical breaking formulations. The dissipation is distributed in proportion to the energy at each frequency (as in the phase-averaged model) or as a function of frequency [Mase and Kirby, 1992]. Boussinesq models can reproduce the spectral evolution of two-peaked spectra in the surf zone [Chen *et al.*, 1997]. Chen *et al.* [1997] show that the larger loss of energy in the high-frequency peak is due to large nonlinear energy transfers to other parts of the spectrum. They also note that the resulting surf zone spectra generated by the Boussinesq model are insensitive to the form of the surf zone dissipation function (however, wave skewness and kurtosis are affected by the choice of the dissipation function). This implies that the nonlinear three-wave interactions in the surf zone quickly readjust any inaccuracies in spectra shape caused by an incorrect dissipation function. Using a Boussinesq model, Herbers *et al.* [2000] show that decay in the spectral peak results primarily from nonlinear energy transfers to higher frequencies, where it is apparently dissipated. They also suggest that this nonlinear energy cascade is similar to the energy balance in deepwater waves.

[6] Both Eldeberky and Battjes [1996] and Herbers and Burton [1997] show numerical Boussinesq simulations (Eldeberky and Battjes also include consistent lab measurement) of spectra that evolve from sharp harmonics and steep high-frequency slopes to flatter, smoother high-frequency tails in shallow water. Herbers and Burton [1997, p. 21,102] report "the principle effects of the nonlinear interactions is to distribute energy equally across the spectrum" and both narrow and broad spectra evolve to "similar broad, almost featureless spectra" in shallow water. Neither paper addressed parameterization of this broad, featureless region.

[7] The concept of spectral equilibrium ranges has proven valuable in phase-averaged numerical modeling of wave generation and transformation. With the exception of Thornton [1977] and Zakharov [1999], equilibrium ranges

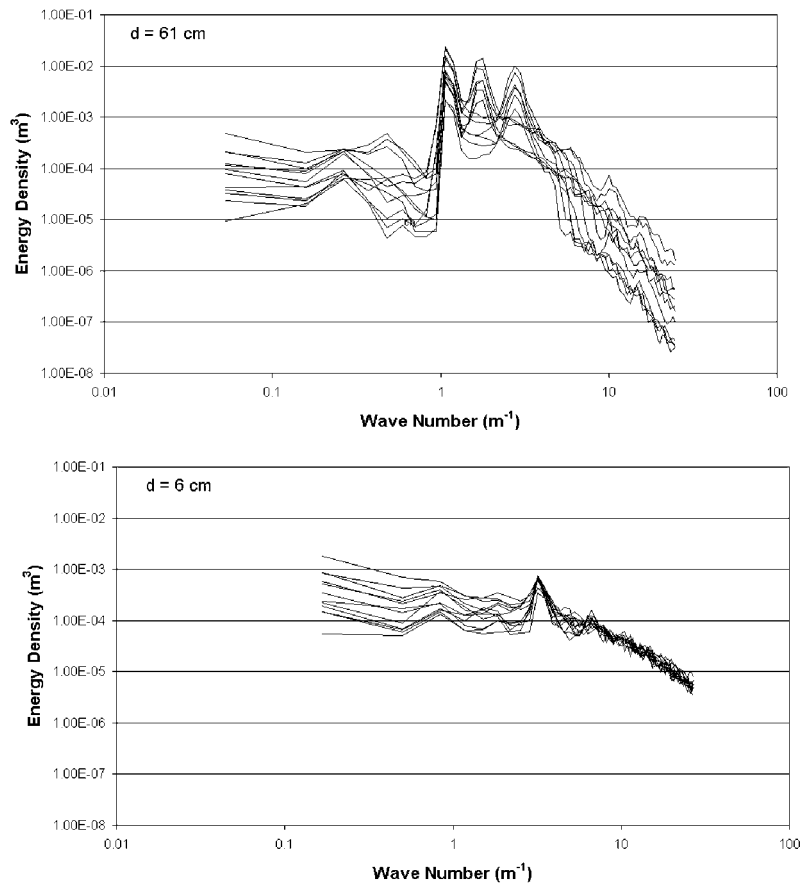


Figure 2. Evolution of double-peaked lab spectra from depth of (top) 61 cm to (bottom) 6 cm.

have been ignored in the surf zone. In the surf zone, spectral shape has been modeled through two approaches: (1) simple linear transformation that inaccurately preserves the spectral shape outside the surf zone and (2) significantly more complex Boussinesq models. In this paper we use laboratory and field data to show that the equilibrium range shape in the surf zone is $k^{-5/2}$ for values of kd greater than approximately unity. Where the equilibrium range extends to values of kd less than unity, the slope of the equilibrium range of the spectrum is flatter than $k^{-5/2}$. The slope in this inner region is approximately $k^{-4/3}$, equivalent to that derived by *Zakharov* [1999].

2. Equilibrium Range Power Laws for Laboratory Spectra

2.1. Laboratory Data

[8] Two laboratory data sets were used to investigate equilibrium ranges in surf zone wave spectra. The laboratory data were collected in a flume at the ERDC Coastal and Hydraulics Laboratory. Descriptions of the data collection are provided below.

[9] *Davis et al.* [1991] and *Smith and Vincent* [1992] measured wave shoaling and breaking on a 1:30 slope in a 0.46-m-wide, 45.7-m-long, and 0.9-m-deep wave flume. Incident waves were generated with a TMA spectral shape, peak wave periods ranging from 1.25 to 2.5 sec, and zero-moment wave heights (H_s) from 0.03 to 0.15 m. The Smith and Vincent experiment included single and double peaked

spectra (1.25/2.5 sec and 1.75/2.5 sec) and the *Davis et al.* test were single peaked. Nine surface-piercing, electrical resistance gauges were used to measure the variation of the free surface in water depths of 0.61 to 0.03 m. The gauges were sampled at 10 Hz for 1250 sec. The first 30 sec of data were truncated to allow waves to propagate through the gauge array. Spectra were estimated from zero-meaned, 10% cosine bell windowed wave records with band averaging. Resulting resolution bandwidth is 0.042 Hz and spectral estimates have a nominal 60 degrees of freedom. The *Davis et al.* data set consists of 270 measured spectra (30 incident wave cases at nine gauges), and the *Smith and Vincent* data set consists of 189 measured spectra (21 incident wave cases at nine gauges).

2.2. Spectral Parameterization

[10] The laboratory data of *Smith and Vincent* [1992] were investigated first. The data demonstrated that multi-peaked wave spectra evolved to have a single peak in the surf zone, consistent with the field data in Figure 1. Moreover the data indicate that within the surf zone, the spectra evolved to a quasi-equilibrium shape irrespective of the initial condition as long as the offshore spectra had the same low wave number peak (Figure 2). Figure 2 (top) shows that the initial spectra (depth of 61 cm) vary over a range of two decades in energy density. Figure 2 (bottom) is the spectra of the same waves after shoaling and breaking. The spectra are shifted to higher wave numbers because of the effect of decreased depth in the dispersion relationship. The effects

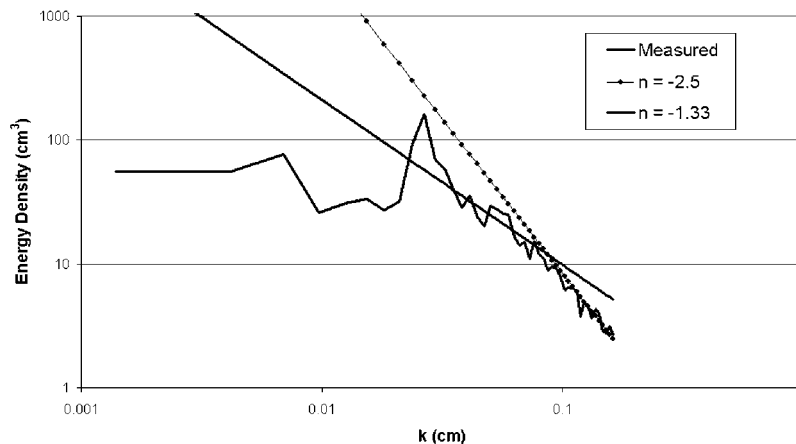


Figure 3. Example of Toba equilibrium range ($n = -5/2$) fit to lab data ($d = 18.3$ cm).

of shoaling and breaking are two fold: (1) high-frequency peaks are eradicated and (2) the wide range of energy densities at high wave numbers collapse toward an almost universal spectral equilibrium range. In the surf zone (depth of 6 cm; Figure 2 (bottom)), the spectra are within a third of a decade about the mean. The variability at the peak is not large (40% versus a factor of up to 5 in the initial conditions). Most variability is seen in the low-frequency range of the spectra that corresponds to infragravity bands in field spectra, and may indicate tank oscillation in the lab. The lower-frequency or infragravity region of the spectrum is not considered in this paper. Thus the trends of the laboratory spectra are consistent with the general description given by *Herbers and Burton* [1997].

[11] Working in wave number space and analyzing the surf zone spectra indicated that the high-wave number components could be fit by the $n = -2.5$ (equation (1)) equilibrium range (Figure 3). The $n = -2.5$ range will be referred to as the Toba range, on the basis of *Toba* [1973]. However, in examination of the data it was clear that as the water became progressively shallower this equation did not describe the entire high-frequency range, and a second range with a flatter slope developed for kd less than approximately unity. *Zakharov* [1999] suggested $n = -4/3$ is valid for small kd . This range will be referred to as the

Zakharov range. As the depth became progressively shallower, this range occupied a larger portion of the total equilibrium range. Using linear regression, the exponent n (equation (1)) was determined for the range $k = 2.5 k_p$ to $k = 1/d$ and for $k > 1/d$ for the measured lab data at the shallowest gauge ($d = 0.06$ cm). The average exponents for the 12 cases were $n = -1.57$ ($kd < 1$) and $n = -2.42$ ($kd > 1$). Figure 4 shows the average compensated spectra for these 12 cases, where the compensated spectrum is defined as $F(k) k^{-n}$. In the region where the given n is valid ($kd < 1$ for $n = -1.57$ and $kd > 1$ for $n = -2.42$), the compensated spectrum is approximately horizontal. The exponent for upper equilibrium range components is close to the previously documented value of $n = -2.5$ for deep and intermediate water depths, and the value for the lower equilibrium range is slightly higher than the theoretical value given by *Zakharov* [1999].

[12] We performed similar analyses with the single peak lab data of *Davis et al.* [1991]. Limiting analysis to only surf zone spectra (defined here as wave-height-to-water-depth ratio greater than 0.4), the average Zakharov range coefficient was found to be $n = -1.26$ (standard deviation of 0.31) and the Toba range coefficient was found to be $n = -2.56$ (standard deviation of 0.36). Exponents were only calculated for cases with at least 10 points in the

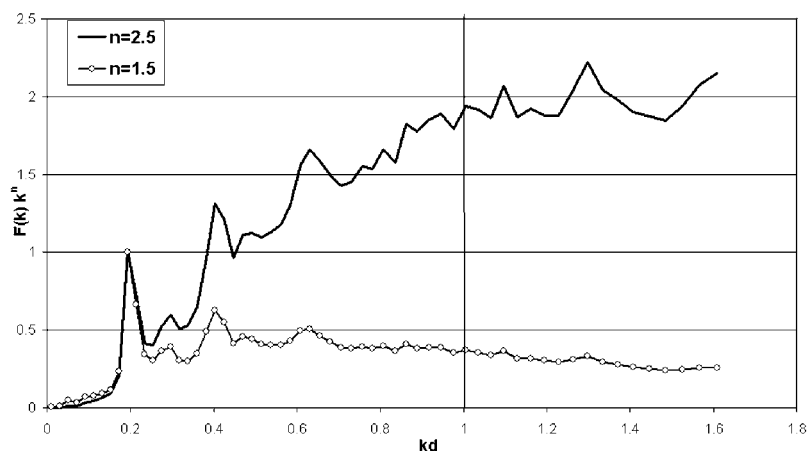


Figure 4. Example both Toba and Zakharov ranges fit to lab data ($d = 7.2$ cm).

equilibrium range. Twenty-eight spectra were used to calculate the Zakharov range and 39 for the Toba range. With this somewhat larger and more diverse data set, the exponents are closer to the theoretical values.

[13] The following mathematical model describes the spectral equilibrium range (for $k > 2.5 k_p$):

$$\begin{aligned} F(k) &= \beta_{\text{Zak}} k^{-4/3} \text{ for } kd < 1 \\ F(k) &= \beta_{\text{Toba}} k^{-5/2} \text{ for } kd \geq 1 \end{aligned} \quad (3)$$

where β_{Zak} and β_{Toba} are dimensional equilibrium range coefficients that will be discussed in section 4. This form can be generalized to the entire wind wave spectrum with a TMA-like form by multiplying by the JONSWAP and Pierson-Moskowitz shape functions. Approximately 20–30% of the energy in the shallow-water spectra was at wave numbers above $2.5 k_p$.

[14] The laboratory data suggest the following conceptual model. As waves with a single or multipeak wave spectrum enter the surf zone their spectra rapidly evolve to a single peak spectrum whose peak is that of the lowest distinct peak in the offshore spectrum. In shallow water depths, the spectra develop two slopes in the equilibrium range. In the multipeak case this is at the expense of the higher-frequency peak. This equilibrium range is not sensitive to the initial spectral shape, but appears coupled to local water depth. As the waves enter shallower water, progressively more of the equilibrium range is described by the Zakharov range, with the Toba range valid only at wave numbers of $k > 1/d$.

[15] When the waves are near breaking, strong harmonics temporarily develop, but appear to be largely a perturbation about the equilibrium range. As the waves progress further into the surf zone the harmonics are diminished (similar to *Herbers and Burton [1997]*). The laboratory cases were generated to have spectral widths that were not extremely narrow, but representative of typical wind seas or swell.

[16] The laboratory data provoked a series of questions: 1) Does the model hold for ocean waves shoaling and breaking on natural beaches? 2) What parameters do the equilibrium range coefficients (β_{Zak} and β_{Toba}) relate to in the surf zone, and how does β_{Toba} transition from outside the surf zone, where it can be directly related to wind, to its value inside the surf zone? 3) Can the transition point from one subrange of the equilibrium range to the other be better specified?

3. Extending Parameterizations With Field Data

[17] Two field data sets were used to evaluate equilibrium ranges in nearshore wave spectra. The field data were collected at the ERDC FRF in Duck, North Carolina. The FRF is located on the Atlantic coast of the United States. Descriptions of the data collection and analyses are given in the following sections.

3.1. Field Data

3.1.1. Baylor Gauge Data

[18] The first source of field data is a Model 23766 Baylor gauge (Baylor Co., Houston, TX), a surface piercing, impedance wire sensor that is mounted beneath the

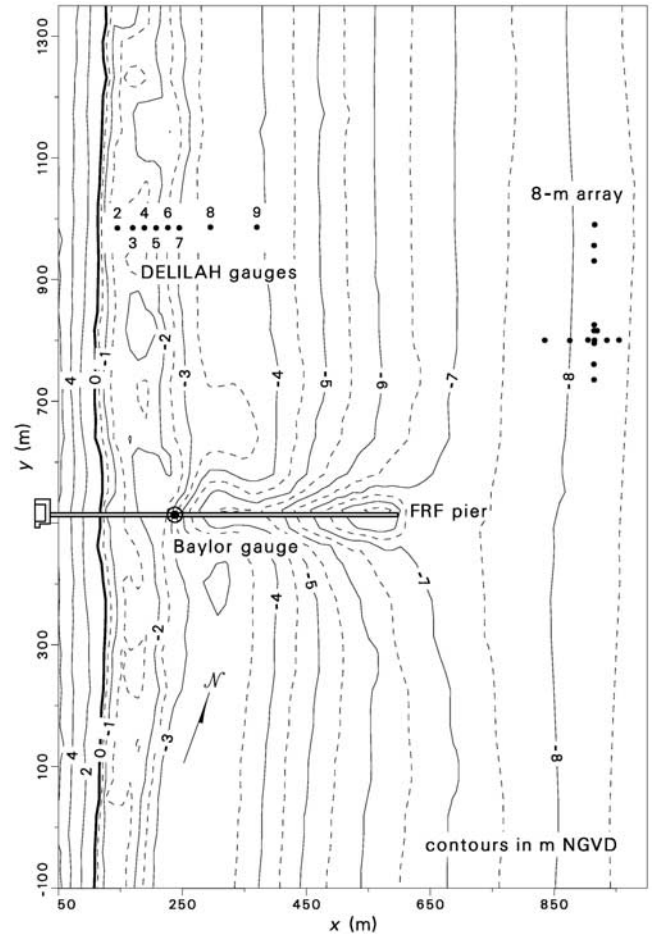


Figure 5. Wave measurement locations at the FRF, Duck, North Carolina.

FRF pier, about 150 m offshore in approximately 3-m depth (Figure 5). The gauge responds well to swell and wind seas at frequencies less than about 0.5 Hz and is one of the permanent suite of instruments maintained by the FRF. The FRF data archive for this gauge contains frequency spectra based on 2048-s records of data sampled at 2 Hz. These spectra are computed via Fourier analysis of 15 half-lapped, demeaned, and windowed (10% cosine taper) data segments of 256-s duration, with no band averaging. Resulting degrees of freedom are at least 16 (based on the eight contiguous segments that constitute a record, with a few more degrees of freedom possible from the lapped segments). To increase degrees of freedom for the present study, archived spectra from four contiguous 2048-s records (spanning about 2 hour 16 min) were averaged, and these results were smoothed in groups of three frequency bands. Final spectral estimates have a minimum of 192 degrees of freedom in 42 discrete bands of width 0.0117 Hz extending to 0.4883 Hz.

[19] For conversion of frequency to wave number and transformation of frequency spectra to wave number spectra via the linear dispersion relation, it is necessary to know water depth. Baylor gauge mean readings were unreliable for this purpose, so water depth estimates were made by adding tidal elevation relative to NGVD (the 1929 National Geodetic Vertical Datum) to seafloor location below NGVD

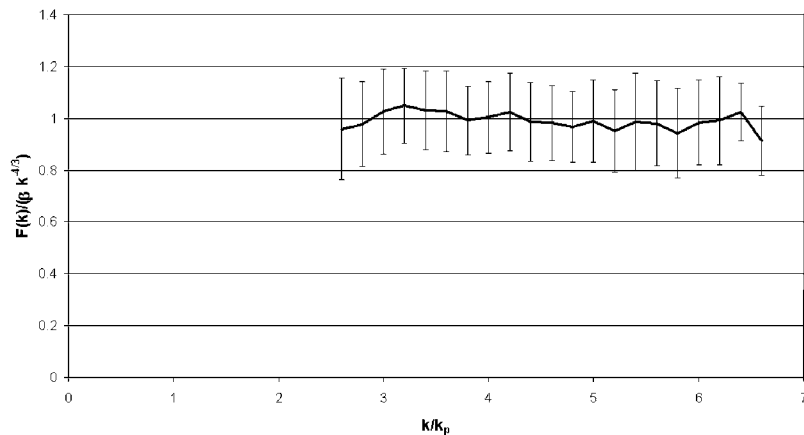


Figure 6. Averaged compensated spectra for DELILAH data ($H_s/d > 0.4$) for $k/k_p > 2.5$ and $kd < 1$ (Zakharov range).

at the Baylor site. Tidal elevation was estimated as the median of mean water levels relative to NGVD measured by the 15 pressure gauges of the 8-m array (Figure 5), which were averaged over the same duration as a Baylor spectral estimate. Bottom location at the Baylor site was estimated by interpolating pier soundings conducted monthly by the FRF. The working data set of Baylor spectra used here is based on samples at and around the peaks of 29 storm events that occurred at the FRF between October 1986 and April 1991 as identified by Long [1994]. Of the sample times identified, a total of 417 cases were found where the gauge and data collection system were functioning, and the data were free of identifiable noise above the digitization noise floor. Of these cases, 133 had height-to-depth ratios exceeding 0.4 (average depth of 2.7 m) and were used for further analysis.

3.1.2. DELILAH Pressure Array Data

[20] In October of 1990 the Duck Experiment on Low-frequency and Incident-band Longshore and Across-shore Hydrodynamics (DELILAH) was conducted at the FRF [Thornton *et al.*, 1996; Birkemeier *et al.*, 1997]. DELILAH included a cross-shore array of Setra Model 280E strain gauges (Setra Systems Inc., Boxborough, MA), mounted on pipes jetted into the bottom at locations shown in Figure 6, and hard wired to a data collection system ashore. DELILAH Gauges 2–9 were used in these analyses. The beach slope ranged from approximately 1:100 at the outer gauge to 1:10 on the foreshore at the inner gauge. The middle gauges traversed the nearshore bar and trough. The initial water depths at the gauges ranged from -0.9 to -4.3 m NGVD. Gauge outputs were sampled at 8 Hz virtually continuously for about 20 days. Extracting 8192 s of data (about 2 hour, 16 min) for each gauge at approximately 3-hour intervals provided representative samples for spectral analysis. Pressure data were calibrated to represent a static seawater column of density 1.023 gm/cc. Frequency spectra were found by Fourier analysis of 31 half-lapped, surface-corrected, demeaned, and windowed (full length Kaiser-Bessel window) data segments of 512-s duration, with smoothing over groups of five frequency bands. Resulting resolution bandwidth is 0.009766 Hz and spectral estimates have a nominal minimum of 160 degrees of freedom (based on the 16 contiguous ensembles that constitute a time series).

[21] The data were known to contain 4-s gaps of spurious information at roughly 20-min intervals owing to the data collection system, and pressure gauge mean values were found to have drift problems [Birkemeier *et al.*, 1997]. Data gaps were avoided by sliding ensemble boundaries earlier or later in a time series so as to surround, but not include, the gaps. At worst, this reduces degrees of freedom to 157. Drifting mean values were replaced by adding surveyed gauge depth below NGVD to tidal elevation above NGVD, the latter being estimated with interpolated 512-s averages of water level above NGVD measured with a Paroscientific Model 245A-101 pressure gauge (Paroscientific Inc., Redmond, WA), compensated for barometric deviation from one standard atmosphere using data from the FRF barometer. The Paroscientific sensor was the third gauge seaward in the cross-shore arm of the 8-m array (Figure 5) during DELILAH. Total water depth was estimated by adding tidal elevation above NGVD to seafloor location below NGVD as found by spatial and temporal interpolation of detailed daily bathymetric surveys of the DELILAH instrument zone [Birkemeier *et al.*, 1997].

[22] Gauge and total water depths were estimated for each ensemble so that raw Fourier transforms could be corrected for frequency- and depth-dependent wave attenuation via the pressure response function of linear wave theory prior to ensemble and band averaging. To avoid amplifying noise in the tail of a spectrum, estimates were truncated for frequencies where the pressure correction factor was greater than 10 (variance correction greater than 100). Sample spectra from DELILAH thus have variable high-frequency cutoffs that depend on the highest tide stage and gauge depth of any included ensemble.

[23] For the spectral analysis used here to be correct, it is necessary that a gauge remain in the water column for the entire sample duration. Results would be compromised if a gauge was buried or exposed to air, and such cases were eliminated from the set presented here. Burial was assumed if gauge depth exceeded water depth within any ensemble. Aerial exposure was assumed if a time series water level equaled gauge elevation within any ensemble. Time series were not surface corrected for this test as gauge exposure would more likely owe to deep troughs of low-frequency (less attenuated) waves. For functioning gauges passing the

Table 1. Estimated Equilibrium Range Exponents Calculated From Measurements

Gauge	Average Depth, m	Zakharov Range			Toba Range		
		n	Standard Deviation	Number of Spectra	n	Standard Deviation	Number of Spectra
Baylor	2.7	-1.51	0.48	53	-2.59	0.40	58
DELILAH 3	1.5	-1.31	0.28	33	-	-	-
DELILAH 4	1.6	-1.31	0.37	48	-	-	-
DELILAH 5	1.7	-1.44	0.38	53	-	-	-
2-Peak Lab	0.06	-1.57	0.36	12	-2.42	0.19	12
1-Peak Lab	0.13	-1.26	0.31	28	-2.56	0.39	39

water column test and with complete records in the imposed sampling scheme, a total of 172 sample spectra were derived from DELILAH observations at Gauges 3–5 with height-to-depth ratios exceeding 0.4 (average depths 1.5 to 1.7 m).

3.2. Equilibrium Range Analysis

[24] The field data provide a wide variety of shallow-water wave spectra for conditions in or near breaking. Linear regression was applied to the field data in a similar manner to the lab data to estimate the exponent in the equilibrium range for the Zakharov and Toba regions. For the Baylor measurements, there were no cases with at least 10 points between $k = 2.5 k_p$ and $1/d$. So for this gauge only, the lower wave number range was relaxed to $1.5 k_p$. In this range for the outer/mid surf zone Baylor measurements, harmonics were often present which bias the equilibrium range exponent estimates. Thus, if harmonics were present (defined as a spectral peak 30% or greater above the local minimum), that region of the spectrum was neglected in the regression calculation (an average of 12% of the points were eliminated). The upper limit of the Toba range was also limited to $6 k_p$. At larger wave numbers, the spectral slope becomes steeper (approximately $n = -3.0$). The DELILAH measurements were made with pressure gauges, so the higher-frequency Toba range is unreliable because amplified noise flattens the slope (or even reverses the slope). The regression results for the field data are given in Table 1. The lab results are repeated for comparison. Overall, the equi-

librium range exponents are very near the Zakharov theoretical value for $kd < 1$ and the Toba deepwater observational value for $kd > 1$.

[25] To examine the overall effectiveness of the fit of equation (3) to the field data, we computed

$$\varphi(k) = F(k)/(\beta k^n) \quad (4)$$

where $n = -4/3$ for the Zakharov range and -2.5 for the Toba range. If equation (3) exactly fit the observed spectrum of all k then $\varphi(k) = 1$. The degree to which the observations are not fit by equation (3) is then shown by $\varphi(k) \neq 1$. By comparing $\varphi(k)$ for each observation, and averaging relative to k/k_p (bins of $0.2 k/k_p$) one can determine where consistent deviations occur. Figure 6 shows the average $\varphi(k)$ for the Zakharov range plotted versus k/k_p along with its standard deviation for $k/k_p = 1$ to 7 for DELILAH Gauges 3–5 (all cases with $H_s/d > 0.4$). This standard deviation is calculated for each $0.2 k/k_p$ bin across 198 measured spectra. More spectra are used for these calculations than appear in Table 1 because we do not require 10 or more points in the equilibrium range to estimate n . Over this range the mean value of $\varphi(k)$ lies close to 1 for data in the Zakharov range. The plot demonstrates that equation (3) provides a good approximation to the overall data set. Figure 7 shows the average $\varphi(k)$ using $n = -2.5$ for the Toba range plotted versus k/k_p along with its standard deviation for $k/k_p = 1$ to 9 for the Baylor Gauge (all cases with $H_s/d > 0.4$) for 134 spectra. The figure shows that the fit deteriorates for k/k_p greater than approximately 6. Because β is calculated for the full range of k/k_p , it is expected that $\varphi(k)$ is slightly larger than 1 for the lower range to balance the small value of $\varphi(k)$ in the upper range. Figure 7 also shows the fit for $n = -3$. For k/k_p between approximately 6 and 8.5, $n = -3$ provides a better fit to the measured spectra. The standard deviation for $n = -3$ is not plotted in Figure 7, but is the same magnitude as shown for $n = -2.5$ (approximately 0.15).

[26] The field data support the initial conclusions from the laboratory data. Active surf zone wave spectra ($H_s/d > 0.4$) show two distinct subranges in the equilibrium range that can be approximated by equation (3), as long as $k_p d \ll 1$

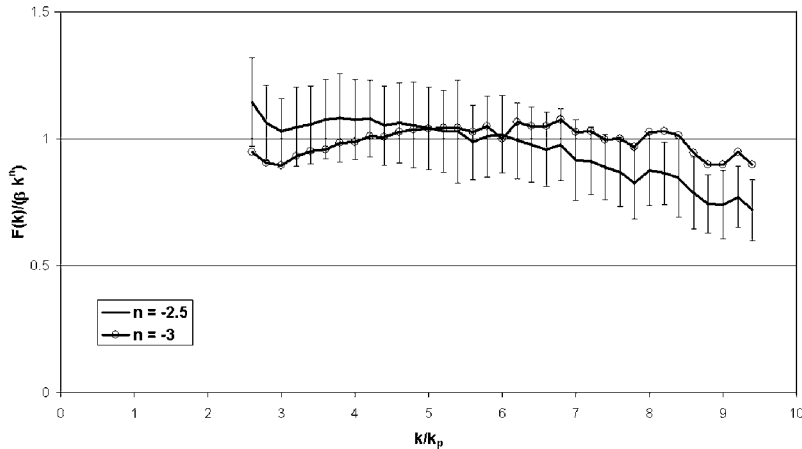


Figure 7. Averaged compensated spectra for Baylor data ($H_s/d > 0.4$) for $k/k_p > 2.5$ and $kd > 1$ (Toba range).

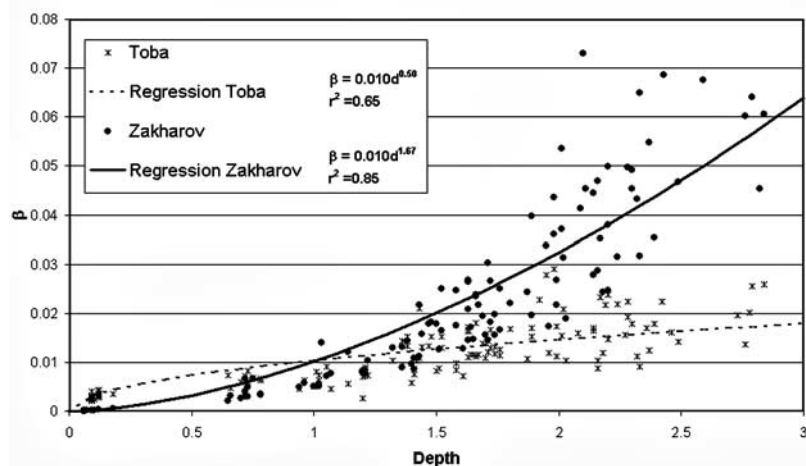


Figure 8. Parameterization of β_{Toba} and β_{Zak} as a function of d .

(if $k_p d > 1$, only the Toba range exists). The Baylor data also suggest that at larger values of k , the spectral slope steepens to k^{-3} .

4. Equilibrium Range Coefficients

[27] Outside of the surf zone and in deep water, the coefficient β (equation (1)) for the equilibrium range has been shown to be of the form [Kitaigorodskii, 1983; Miller and Vincent, 1990]

$$\beta = \alpha U_{10} g^{-1/2} \quad (5)$$

where U_{10} is the wind speed referenced at 10 m above the water, and α has values in the range 0.002–0.003 [Resio, 1988; Miller and Vincent, 1990]. For surf zone spectra, the coefficients β_{Zak} and β_{Toba} were estimated from field and laboratory data by fitting equation (3) to each spectrum to obtain the best fit β values.

[28] The β coefficients must have dimensions to satisfy the power law equations. β_{Toba} has the same dimensions as equation (5) ($\text{length}^{1/2}$), and β_{Zak} has the dimensions ($\text{length}^{5/3}$). It is unlikely that wind speed is appropriate for the surf zone, because the surf zone is narrow and there is little time or space for the wind to act on the waves. Moreover the laboratory data were mechanically generated with a paddle and wind speed is not relevant. The parameters of importance in the surf zone include water depth, wave height, and peak period. Wave height and β are dependent quantities, and peak period is generally considered weakly related to surf zone energy. Thus water depth is the obvious choice to relate to β . Figure 8 shows β_{Toba} as function of d . The resulting regression for β_{Toba} is

$$\beta_{\text{Toba}} = \alpha_{\text{Toba}} d^{0.50} \quad (6)$$

where $\alpha_{\text{Toba}} = 0.0103$ and the correlation coefficient (r^2) is 0.65. Figure 8 also shows β_{Zak} as function of d . The resulting regression is

$$\beta_{\text{Zak}} = \alpha_{\text{Zak}} d^{1.67} \quad (7)$$

where $\alpha_{\text{Zak}} = 0.0102$ and the correlation coefficient is 0.85. Letting the exponents on d float in the regression analyses gives exponents of 0.53 ($r^2 = 0.81$) and 1.57 ($r^2 = 0.98$) for the Toba and Zakharov ranges, respectively. These values are close to the dimensionally consistent exponents of 0.50 and 1.67 in equations (6) and (7). The spectra must be continuous at the transition between the Toba and Zakharov regions, estimated as $kd = 1$. To satisfy this constraint, α_{Zak} must equal α_{Toba} , and the regression results give consistent α values. The data used for determining the α values were limited to measurements with $H_s/d \geq 0.6$ to nominally include the saturated breaking zone only (where most of the waves are actively breaking). This includes 138 data points for the Toba range and 164 points for the Zakharov range. In areas of the surf zone where waves are reforming (i.e., in bar troughs or along flat slopes), the local water depth does not limit the energy and the local definition of β (equations (6) and (7)) is not appropriate. This is analogous to determining β in equation (5) for a spatially nonuniform wind field. The energy (or β value) would be calculated from the integrated wind input over the domain, whereas in the surf zone, the β value would result from the integrated impact of breaking over the variable bathymetry. Equations (6) and (7) combined with equation (3) provide a prognostic equation for estimating the surf zone equilibrium range. This formulation was developed using both measurements of ocean waves that were wind generated and laboratory waves that were mechanically generated.

5. Transition to the Surf Zone

[29] We have produced a description of spectra in the surf zone showing the evolution of the equilibrium range as the waves break, eventually producing a structure with two subranges. Resio *et al.* [2001] used intermediate-depth data from FRF gauges (8 and 18 m depth) in their analysis and found that $n = -5/2$ (equation (1)). The coefficient β for a sampling of the 18-m Waverider buoy data is plotted against wind speed U_{10} at the pier end in Figure 9. β is almost linearly dependent upon U_{10}

$$\beta = 0.002 U_{10} g^{-1/2} \quad (8)$$

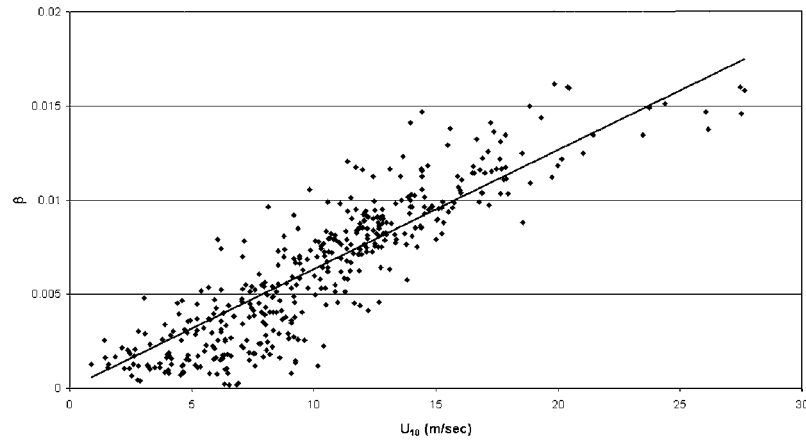


Figure 9. Linear relationship of β as a function of wind speed (U_{10}) for the FRF Waverider.

which is consistent with equation (5). Other data at the pier end Baylor gauge (8-m depth) show a similar relationship to U_{10} .

[30] When β_{Toba} is estimated from an essentially overlapping set of spectra observed at the Baylor in 3 m of water that is more often in the surf zone, no strong relationship between β_{Toba} and U_{10} is evident as shown by Figure 10. Thus in the 300 m in distance between the end of the pier and the midpier Baylor and 4-m depth change between the two sites, the equilibrium range becomes uncoupled from the wind and appears controlled by depth. With the onset of depth-induced breaking, the dynamics of the spectrum radically shift. We note that in spite of this decoupling, the equilibrium range at the higher wave numbers ($kd > 1$) retain the $k^{-5/2}$ shape.

6. Discussion

[31] Field and laboratory observations in the surf zone show evidence of an equilibrium range that has some similarities to wave spectra outside of the surf zone. The spectra have a monotonic decline in value away from the peak on which harmonics are sometimes a deviation; analogous to the offshore cases it appears readily formulated in terms of a power law in wave number, and the saturation level (equilibrium range coefficient β) is not universal, but

is dependent on local geophysical or oceanographic conditions. However, in contrast to offshore spectra, the equilibrium range is divided into two separate subranges that we have termed the Zakharov and Toba ranges, with the Toba range having the same power law dependence as the offshore equilibrium range. The subrange transition is near a kd value of unity. The transition at $kd = 1$ is determined here purely by observation. Theory would suggest that the transition would occur over a wide range of kd instead of a single point (Zakharov suggested an upper limit for of $kd = 0.3$ for the lower range). At larger wave numbers and deeper relative depths, a third region with a shape of k^{-3} is sometimes observed in the data set.

[32] Contrary to the offshore case, the equilibrium range coefficients are not a function of wind speed but are related to water depth. The strength of the processes that mold these subranges would appear to be great for two reasons. First the transition is rapid: in the laboratory (1:30 slope) this transition takes place over a few meters and at the Toba transition may be of order the deepwater wavelength of waves at the dominant period; in time the span is of the order of a few wave periods of the dominant wave. Second, as shown by the dual peak lab data, the transition can eradicate wave trains with offshore energy levels that differ by two to three orders of magnitude and arrive at the same apparently depth-limited conditions. The spectral evolution

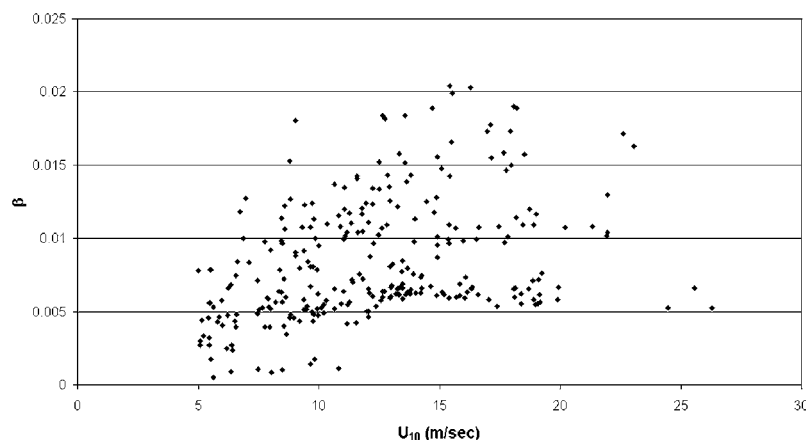


Figure 10. Relationship of β as a function of wind speed (U_{10}) for 4-m Baylor.

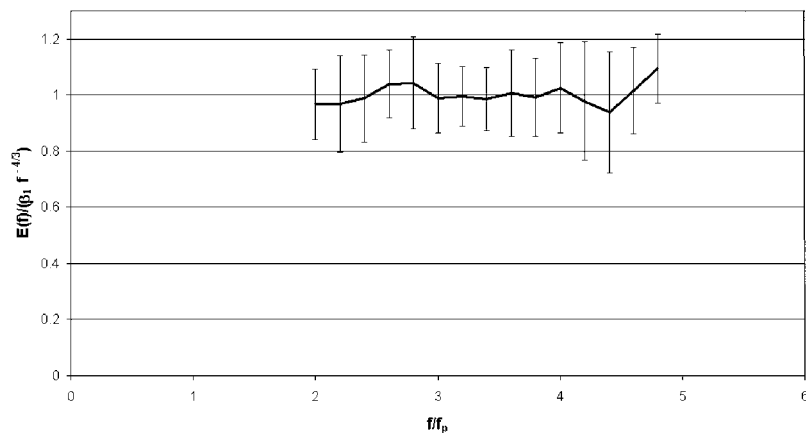


Figure 11. Averaged compensated spectra for DELILAH data expressed in frequency space ($H_s/d > 0.4$) for $k/k_p > 2.5$ and $kd < 1$ (Zakharov range).

is consistent for unidirectional laboratory flume measurements and multidirectional field measurements.

[33] In the surf zone, wave nonlinearity is strong, which feeds the energy cascade from the spectral peak to high frequencies. *Elgar et al.* [1990] and *Norheim et al.* [1998] performed numerical experiments with Boussinesq models to examine the spectral evolution in shallow water over many wavelengths. *Elgar et al.* [1990] state that after approximately 30 wavelengths (on a flat bottom), the power spectra is broad and the spectral peak and harmonics are gone. Our examination of their Figure 8 shows the spectra evolve to approximately the Zakharov equilibrium range shape after 30 wavelengths (kd is less than 1) and remain approximately constant through the 70 wavelengths of their calculations. Examples provided by *Norheim et al.* show that lower energy spectra ($H/d = 0.033$) do not reach the equilibrium, but higher-energy waves ($H/d = 0.3$) do appear to evolve to the equilibrium shape. These examples are all outside the surf zone. For cases of a surf zone with extremely flat slope, it isn't clear if the equilibrium ranges proposed in the paper would persist after breaking ceases (certainly the coefficients in equations (6) and (7) would be less, as dissipation from sources other than wave breaking define the wave height).

[34] Although the equilibrium range described by the parameterization represents 20–30% of the wave energy, there are two reasons for getting this portion correct. First, in many existing spectral models, the wave energy in this region can be significantly overestimated especially in the case of dual peak wave spectra, with attendant misestimates of radiation stress. Second, the ability of an advanced model (whether Boussinesq, Hamiltonian or other) to correctly represent wave dynamics can be judged by its ability to correctly reproduce this region, especially as waves pass from the region of direct wind forcing outside the surf zone to the region dominated by swash zone dynamics near the shoreline.

[35] In our analyses we have used a time-based FFT to analyze the Fourier modes of the surface elevation (or pressure) record. In the case of the pressure records we have used widely accepted linear theory-based transfer functions to convert the pressure spectra into an estimation of the elevation spectrum. When we mathematically transform these frequency spectra in to wave number spectra and

transform the frequency coordinate to its linear wave number equivalent, we find that the spectra obey power laws in k both inside and outside the surf zone. We are not asserting that any of these higher-wave number Fourier modes are free (or for that matter bound) linear waves. Figure 11 shows the fit of the Zakharov range expressed in frequency space, which does not require the linear transfer function. The fit is similar to that given in wave number space in Figure 6. This suggests that the linear calculation of wave number does not bias the results.

[36] Our visual observation of the waves and our examination of many wave train records from the lab and field suggest that as one of the longer, larger waves in the record shoals and approaches breaking, higher-wave number modes grow and are in-phase at the crest. As the waves break, it is these components that disappear. This may be analogous to what *Herbers et al.* [2000] calculate with their Boussinesq code. We also note that the theoretical derivation for the Zakharov range and the Toba range both rely on a constant flux of energy out of the peak region to some high-wave number region where it is dissipated. We believe what our analyzes show is that these ephemeral in time and space components in the average over a 20–40 min (in the field) wave record follow the simple power laws shown. *Herbers et al.*'s calculations suggest that the transfers to high wave numbers are large enough to explain most of the decay in the primary wave components, and argues that the actual dissipation is then at high wave numbers. Explicit calculations of four-wave interaction components of the transfer rate would be interesting to see if it too shows enough transfer away from the dominant peak or whether dissipation is needed at the peak.

[37] The original motivation for the research reported in this paper was to improve the prediction of wave spectra in the surf zone especially for the case of dual peak spectra in linear, phase-averaged engineering models. The equilibrium range formulation described here appears to offer the potential for a simple approximation that yields spectral shapes consistent to that observed in the laboratory and field. Issues not fully resolved are the complete range of applicability (i.e., bottom slope, wave steepness) and an improved understanding of the equilibrium subrange coefficients. We note that modern Boussinesq models appear to represent the essentials of this behavior with the additional advantage of

predicting the infragravity band of the spectrum as well as the higher moments. This is however at a significantly higher computational burden. The equilibrium range concept also offers the possibility of parameterizing the high-frequency portion of Boussinesq model calculations.

7. Summary

[38] Laboratory and field data show the existence of two distinct equilibrium ranges in surf zone wave spectra. The Toba range ($k > 1/d$) has the form $k^{-5/2}$, which is the same form identified in deep and finite depth water [Toba, 1973; Kitaigorodskii, 1983; Resio *et al.*, 2001]. The second equilibrium range has the form $k^{-4/3}$ and occurs for $k < 1/d$. Zakharov [1999] derived an equivalent form of this range (in terms of ω) for very shallow depths. There is also evidence of a k^{-3} range [Phillips, 1958] at higher frequencies that was not investigated in depth in this paper. The equilibrium range coefficients in both the Toba and Zakharov ranges are a function of the water depth. Equations (3), (6), and (7) define the equilibrium ranges and coefficients. For the purposes of this paper the surf zone implies waves with $k_p d \ll 1$ and $H_s/d > 0.4$.

[39] The data sets used in these analyses covered a large range of conditions: two orders of magnitude in wave height, one order of magnitude in peak period, unidirectional (flume) and multidirectional (field), single and multiple spectral peaks, wind and mechanical generation, and plane and barred beaches. Typically the slopes were from 1:100 to 1:30. For these vastly different conditions, the equilibrium ranges were consistent, providing a robust parameterization of equilibrium range of surf zone wave spectra.

[40] **Acknowledgments.** We acknowledge the Chief of Engineers, U.S. Army Corps of Engineers, for permission to publish this paper. Support for JMS was provided through the Transformation-Scale Waves work unit of the U.S. Army Corps of Engineers Navigation Systems Program. The authors gratefully acknowledge the FRF and Ed Thornton for providing the wealth of field data from the FRF archives and the DELILAH experiment. Chuck Long provided analysis of the FRF field data. We thank Don Resio, Vladimir Zakharov, and Chuck Long for helpful discussions.

References

Birkemeier, W., C. Donoghue, C. E. Long, K. K. Hathaway, and C. Baron, The 1990 DELILAH nearshore experiment: Summary report, *Tech. Rep. CHL-97-24*, U.S. Army Eng. Waterw. Exp. Stn., Vicksburg, Miss., 1997.

Booij, N., R. C. Ris, and L. H. Holthuijsen, A third-generation wave model for coastal regions, *J. Geophys. Res.*, *104*, 7649–7666, 1999.

Chen, Y., R. T. Guza, and S. Elgar, Modeling spectra of breaking surface waves in shallow water, *J. Geophys. Res.*, *101*, 1253–1264, 1997.

Davis, J. E., J. M. Smith, and C. L. Vincent, Parametric description for a wave energy spectrum in the surf zone, *Misc. Pap. CERC-91-11*, U.S. Army Eng. Waterw. Exp. Stn., Vicksburg, Miss., 1991.

Donelan, M. A., J. Hamilton, and W. H. Hui, Directional spectra of wind-generated waves, *Philos. Trans. R. Soc. London, Ser. A*, *315*, 509–562, 1985.

Eldeberky, Y., and J. A. Battjes, Spectral modeling of wave breaking: Application to Boussinesq equations, *J. Geophys. Res.*, *101*, 1253–1264, 1996.

Elgar, S., M. H. Freilich, and R. T. Guza, Recurrence in truncated Boussinesq models for nonlinear waves in shallow water, *J. Geophys. Res.*, *95*, 11,547–11,556, 1990.

Hasselmann, K., On the non-linear energy transfer in a gravity wave spectrum, part 1, General theory, *J. Fluid Mech.*, *12*, 481–500, 1962.

Herbers, T. H. C., and M. C. Burton, Nonlinear shoaling of directionally spread waves on a beach, *J. Geophys. Res.*, *102*, 21,101–21,114, 1997.

Herbers, T. H. C., N. R. Russnogle, and S. Elgar, Spectral energy balance of breaking waves within the surf zone, *J. Phys. Oceanogr.*, *30*, 2723–2737, 2000.

Herterich, K., and K. Hasselmann, A similarity relation for the nonlinear energy transfer in a finite-depth gravity-wave spectrum, *J. Fluid Mech.*, *97*, 215–224, 1980.

Kitaigorodskii, S. A., On the theory of the equilibrium range in the spectrum of wind-generated gravity waves, *J. Phys. Oceanogr.*, *13*, 816–827, 1983.

Long, C. E., Storm evolution of directional seas in shallow water, *Tech. Rep. CERC-94-2*, U.S. Army Eng. Waterw. Exp. Stn., Vicksburg, Miss., 1994.

Mase, H., and J. T. Kirby, Hybrid frequency-domain KdV Equation for random wave transformation, *Coastal Engineering 1992: Proceedings of the Twenty-Third International Conference*, edited by B. L. Edge, pp. 474–487, Am. Soc. of Civ. Eng., Reston, Va., 1992.

Miller, H. C., and C. L. Vincent, FRF spectrum: TMA with Kitaigorodskii's f^{-4} scaling, *J. Waterw. Port Coastal Ocean Eng.*, *116*, 57–78, 1990.

Norheim, C. A., T. H. C. Herbers, and S. Elgar, Nonlinear evolution of surface wave spectra on a beach, *J. Phys. Oceanogr.*, *28*, 1534–1551, 1998.

Phillips, O. M., The equilibrium range in the spectrum of wind-generated waves, *J. Fluid Mech.*, *4*, 426–434, 1958.

Phillips, O. M., *Dynamics of the Upper Ocean*, Cambridge Univ. Press, New York, 1966.

Resio, D. T., Shallow-water waves. I: Theory, *J. Waterw. Por. Coastal Ocean Eng.*, *113*, 264–281, 1987.

Resio, D. T., Shallow-water waves. II: Data comparisons, *J. Waterw. Por. Coastal Ocean Eng.*, *114*, 50–65, 1988.

Resio, D. T., J. H. Pihl, B. A. Tracy, and C. L. Vincent, Nonlinear energy fluxes and the finite depth equilibrium range in wave spectra, *J. Geophys. Res.*, *106*, 6985–7000, 2001.

Smith, J. M., and C. L. Vincent, Shoaling and decay of two wave trains on a beach, *J. Waterw. Por. Coastal Ocean Eng.*, *118*, 517–533, 1992.

Smith, J. M., A. R. Sherlock, and D. T. Resio, STWAVE: Steady-state spectral wave model; user's manual for STWAVE, version 3.0, *Spec. Rep. ERDC/CHL SR-01-1*, U.S. Army Eng. Res. and Dev. Cent., Vicksburg, Miss., 2001.

Thornton, E. B., Rederivation of the saturation range in the frequency spectrum of wind-generated gravity waves, *J. Phys. Oceanogr.*, *7*, 137–140, 1977.

Thornton, E. B., H. T. Humiston, and W. Birkemeier, Bar/trough generation on a natural beach, *J. Geophys. Res.*, *101*, 12,097–12,110, 1996.

Toba, Y., Local balance in the air-sea boundary processes on the spectrum of wind waves, *J. Oceanogr. Soc. Jpn.*, *29*, 209–220, 1973.

Zakharov, V., Statistical theory of gravity and capillary waves on the surface of a finite-depth fluid, *Eur. J. Mech. B Fluids*, *18*, 327–344, 1999.

Zakharov, V. E., and N. Filonenko, The energy spectrum for stochastic oscillation of a fluid's surface, *Dokl. Akad. Nauk*, *170*, 1292–1295, 1966.

J. M. Smith, U.S. Army Engineer Research and Development Center, 3909 Halls Ferry Road, CEERDC-HC-C, Vicksburg, MS 39180-6199, USA. (jane.m.smith@erdc.usace.army.mil)

C. L. Vincent, Office of Naval Research, Coastal Dynamics Program, ONR Code 321CD, Office of Naval Research, 800 North Quincy Street, Arlington, VA 22217, USA. (vincenc@onr.navy.mil)